Journal of Computational Mathematics
Vol.29, No.3, 2011, 243–260.

http://www.global-sci.org/jcm
doi:10.4208/jcm.1010-m3069

GALERKIN BOUNDARY NODE METHOD FOR EXTERIOR NEUMANN PROBLEMS*

Xiaolin Li
College of Mathematics Science, Chongqing Normal University, Chongqing 400047, China
Email: lxlmath@163.com
Jialin Zhu
College of Mathematics and Physics, Chongqing University, Chongqing 400044, China
Email: jlzhu@cqu.edu.cn

Abstract

In this paper, we present a meshless Galerkin scheme of boundary integral equations (BIEs), known as the Galerkin boundary node method (GBNM), for two-dimensional exterior Neumann problems that combines the moving least-squares (MLS) approximations and a variational formulation of BIEs. In this approach, boundary conditions can be implemented directly despite the MLS approximations lack the delta function property. Besides, the GBNM keeps the symmetry and positive definiteness of the variational problems. A rigorous error analysis and convergence study of the method is presented in Sobolev spaces. Numerical examples are also given to illustrate the capability of the method.

Mathematics subject classification: 65N12, 65N30, 65N38.
Key words: Meshless, Galerkin boundary node method, Boundary integral equations, Moving least-squares, Error estimate.

1. Introduction

Meshless (or meshfree) methods for numerical solutions of boundary value problems have attracted much attention in recent years [1,2]. Compared to the finite element method (FEM) and the boundary element method (BEM), the main objective of this type of method is to get rid of, or at least to alleviate, the difficulty of meshing and remeshing the entire structure by simply adding or deleting nodes. Meshless methods have been found to have special advantages on problems to which the traditional mesh-based methods are difficult to be applied. These include problems with complicated boundary, moving boundary, large deformations, dynamic fracturing, mesh adaptively, and so on. Meshless methods can be categorized into domain type and boundary type. Several domain type meshless methods, such as the element free Galerkin method (EFGM) [1,3], the generalized FEM [4], the particle-partition of unity method [5], the h-p meshless method [6], the reproducing kernel particle method [2] and the finite point method [7] are very promising methods, and their mathematical backgrounds were well investigated.

Boundary integral equations (BIEs) are attractive computational techniques for linear and exterior problems as they can reduce the dimensionality of the original problem by one. Especially for exterior problems, the use of domain type methods requires discretization of the entire exterior, whereas with BIEs only the surface needs to be discretized. The boundary type meshless methods are developed by the combination of the meshless idea with BIEs, such as

* Received March 15, 2009 / Revised version received April 6, 2010 / Accepted September 29, 2010 / Published online February 28, 2011 /

the boundary node method (BNM) [8], the boundary cloud method [9], the hybrid boundary node method [10], the boundary point interpolation method [11], the boundary element-free method [12] and the Galerkin boundary node method (GBNM) [13]. In contrast with the domain type methods, they are superior in treating problems dealing with infinite or semi-infinite domains. However, most boundary type meshless methods found in the literature lack a rich mathematical foundation to justify their use.

The BNM is formulated using the moving least-squares (MLS) approximations [1, 14] and the technique of BIEs. This method exploits the dimensionality of BIEs and the meshless attribute of the MLS. Nevertheless, since the MLS approximations lack the delta function property, the BNM cannot accurately satisfy boundary conditions. The strategy employed in the BNM [8] involves a new definition of the discrete norm used for the construction of the MLS approximations, which doubles the number of system equations.

The GBNM is a boundary type meshless Galerkin method which combines the MLS scheme and a variational formulation of BIEs. Compared with the BNM, boundary conditions in the GBNM can be satisfied directly and system matrices are symmetric. The main difference between the GBNM and the traditional Galerkin BEM is the way in which the shape function is formulated. In the GBNM, the boundary variables are approximated by the MLS technique that only use the boundary nodes, but in the Galerkin BEM, interpolants of the boundary variables are related to the geometry of the elements. The GBNM has been used for Dirichlet problems of Laplace equation [13] and biharmonic equation [15], and for Stokes flow [16]. In this paper, the GBNM is further developed for solving 2-D exterior Neumann problems.

As in many other meshless methods such as the EFGM and the BNM, background cells are used in the GBNM for numerical integration over the boundary. Cells are used for integration only, and have no restriction on shape or compatibility. The topology of cells can be much simpler than that of elements in the BEM or the FEM, since cells can be divided into smaller ones without affecting their neighbours in any way—such is not the case with boundary or finite elements. This feature makes meshless methods especially suited for adaptive procedures [17,18]. When there is no difference between the cell structure and the boundary, error estimates of the GBNM for solving Dirichlet problems have been established [13, 15]. Generally, as the element in the BEM, the cell structure is an approximation of the boundary. In the case of the cell structure is not coincided with the boundary, the error results from the approximation of the boundary by cells needs to be considered. In this paper, based on the preliminary error results of the GBNM for 2-D Dirichlet problems, we give an asymptotic error estimate of the GBNM for 2-D Neumann problems.

The following discussions begin with the brief description of the MLS approximation in Section 2. The formulations of the GBNM for exterior Neumann problems are developed in Section 3. Error estimates are established in Section 4. Section 5 presents regularization procedures for numerical integration. Section 6 provides some numerical results. Section 7 contains conclusions.

2. The Moving Least Squares Method

2.1. Notations

Let Ω be a bounded domain in $\mathbb{R}^2$ of points $\mathbf{x} = (x_1, x_2)$, its boundary Γ assumed to be sufficiently smooth, and let Ω' be the complementary of $\overline{\Omega} = \Omega + \Gamma$.

For any point $\mathbf{x} \in \Gamma$, we use $\Re(\mathbf{x})$ to denote the domain of influence of $\mathbf{x}$. Let $Q_N = \{\mathbf{x}_i\}_{i=1}^N$ be an arbitrarily chosen set of N boundary nodes $\mathbf{x}_i \in \Gamma$. The set Q_N is used for defining a finite open covering $\{\Re_i\}_{i=1}^N$ of Γ composed of N balls $\Re_i$ centered at the points $\mathbf{x}_i$, $i = 1, 2, \cdots, N$, where $\Re_i = \Re(\mathbf{x}_i)$. Assume that there have $\kappa(\mathbf{x})$ boundary nodes that lie on $\Re(\mathbf{x})$. Then, we use the notation $I_1, I_2, \cdots, I_\kappa$ to express the global sequence number of these nodes, and define $\wedge(\mathbf{x}) := \{I_1, I_2, \cdots, I_\kappa\}$. Besides, we use

$$\Re^i := \{\mathbf{x} \in \Gamma : \mathbf{x}_i \in \Re(\mathbf{x})\}, \quad 1 \le i \le N, \tag{2.1}$$

to denote the set of boundary points whose influence domain includes the boundary node $\mathbf{x}_i$.

Let L be the length of Γ, then Γ is a curve having L-periodic parametric representation with respect to the arc-length s,

$$\mathbf{x} = X(s), \quad s \in [0, L]. \tag{2.2}$$

Obviously, $X(s)$ is a mapping from $\mathbb{R}$ into $\mathbb{R}^2$. Denoted by ℓ the continuous order of Γ, then $X(s) \in \left(C^\ell\right)^2$ and $\partial^m X(s)/\partial s^m$ is bounded provided that $m \le \ell$. From (2.2), boundary nodes $\mathbf{x}_i$ can be represented as $\mathbf{x}_i = X(s_i)$, $1 \le i \le N$. Since Γ is closed, we set $s_0 = s_N - L$, then $\mathbf{x}_0 = \mathbf{x}_N$. Denoted by

$$h := \max_{1 \le i \le N} (s_i - s_{i-1}) \quad \text{and} \quad h_i := \left|\overrightarrow{\mathbf{x}_{i-1}\mathbf{x}_i}\right| = |X(s_i) - X(s_{i-1})|,$$

then from the fact that $\partial X(s)/\partial s$ is bounded we deduce $h_i = \mathcal{O}(h)$, $1 \le i \le N$. Thus, the parameter h can be used to measure the nodal spacing.

2.2. The MLS technique

Since the numerical approximations of the MLS starting from a cluster of scattered nodes instead of interpolation on elements, there have many meshless methods based on the MLS method for the numerical solution of differential equations in recent years. Assume that $\mathbf{x} \in \Gamma$, the MLS approximation for a given function v is defined by [13]

$$v(\mathbf{x}) \approx \mathcal{M}v(\mathbf{x}) = \sum_{i=1}^{N} \Phi_i(\mathbf{x}) v_i, \tag{2.3}$$

where $\mathcal{M}$ is an approximation operator, and

$$\Phi_i(\mathbf{x}) = \Phi_i(X(s)) = \begin{cases} \displaystyle\sum_{j=0}^{\bar{\mathfrak{m}}} P_j(s)[\mathbf{A}^{-1}(s)\mathbf{B}(s)]_{jk}, & i = I_k \in \wedge(\mathbf{x}), \\ 0, & i \notin \wedge(\mathbf{x}), \end{cases} \tag{2.4}$$

for $1 \le i \le N$, and the matrices $\mathbf{A}(s)$ and $\mathbf{B}(s)$ being defined by

$$\mathbf{A}(s) = \sum_{k \in \wedge(X(s))} w_k(s)\, \mathbf{P}(s_k)\, \mathbf{P}^{\mathrm{T}}(s_k), \tag{2.5}$$

$$\mathbf{B}(s) = [w_{I_1}(s)\, \mathbf{P}(s_{I_1}), w_{I_2}(s)\, \mathbf{P}(s_{I_2}), \cdots, w_{I_\kappa}(s)\, \mathbf{P}(s_{I_\kappa})], \tag{2.6}$$

in which $\mathbf{P}(s) = [P_0(s), P_1(s), P_2(s), \cdots, P_{\bar{\mathfrak{m}}}(s)]^{\mathrm{T}}$ is a vector of the polynomial basis, $\bar{\mathfrak{m}} + 1$ is the number of monomials in the polynomial basis, w_k denote weight functions which belong to the space $C_0^\alpha(\Re_i)$, $\alpha \ge 0$, and satisfy

$$w_k(s) > 0 \quad \text{and} \quad \sum_{k \in \wedge(s)} w_k(s) = 1.$$

For our subsequent error analysis, the following conditions will be assumed from now on.

Assumption 2.1. *There is a nonnegative integer* $\gamma \leq \ell$ *such that* $\Phi_i(\mathbf{x}) \in C^\gamma(\Gamma)$.

Assumption 2.2. *There are positive integers* $K_1(\mathbf{x}) \geq \bar{\mathfrak{m}}$ *and* $K_2(\mathbf{x})$ *such that for any* $\mathbf{x} \in \Gamma$, *there are at least* $K_1(\mathbf{x})$ *boundary nodes, and at most* $K_2(\mathbf{x})$ *boundary nodes lie on* $\Re(\mathbf{x})$.

Assumption 2.3. *There exist constants* C_{w1} *and* C_{w2} *independent of* h *such that*

$$C_{w1}h^{-j} \leq \left\|\partial^j w_i(s)\right\|_{L^\infty([0,L])} \leq C_{w2}h^{-j}, 0 \leq j \leq \gamma, 1 \leq i \leq N.$$

From [6], if monomials P_j $(0 \leq j \leq \bar{\mathfrak{m}})$ and weight functions w_i $(1 \leq i \leq N)$ are γ-times continuously differentiable, then $\Phi_i \in C^\gamma(\Gamma)$.

Assumption 2.2 is quite natural since, otherwise, as the number of boundary nodes lie on a local area increases, the shape functions tend to be more and more linearly dependent in the local area. Besides, as indicated by Duarte and Oden [6], a necessary condition for the moment matrix $\mathbf{A}(s)$ to be invertible is that there are at least $\bar{\mathfrak{m}}$ nodes covered in the influence domain of every sample point $\mathbf{x} \in \Gamma$. Moreover, Assumption 2.2 indicates that the radii of any boundary point's influence domain can be measured by the parameter h.

We list below some properties of the MLS shape functions Φ_i.

Proposition 2.1. ([2,6]) $\sum_{i=1}^N \Phi_i(\mathbf{x}) = 1$.

Proposition 2.2. ([13]) $\Phi_i(\mathbf{x}) \in C_0^\gamma\left(\Re^i\right)$, $1 \leq i \leq N$.

The following theorem gives an approximation estimate for the MLS approximations, which is central to the convergence proof of the GBNM.

Theorem 2.1. ([13]) *For any* $v(\mathbf{x}) \in H^{m+1}(\Gamma)$, *there exists a constant* C *independent of* h *such that*

$$\|v(\mathbf{x}) - \mathcal{M}v(\mathbf{x})\|_{H^k(\Gamma)} \leq Ch^{m+1-k}\|v(\mathbf{x})\|_{H^{m+1}(\Gamma)}, \qquad 0 \leq k \leq m \leq \gamma, \tag{2.7}$$

where $H^\tau(\Gamma)$, $\tau \in \mathbb{R}$, *means the Sobolev spaces of functions defined on the curve* Γ [19].

3. The GBNM for Exterior Neumann Problems

In this section, we devote our attention to the 2-D Neumann boundary value problem for the Laplace equation. In the GBNM, meshless shape functions are constructed with the MLS technique and are used in a Galerkin setting for the approximation of the weak form of BIEs.

3.1. BIEs and variational formulation

Consider the following exterior Neumann problem

$$\Delta u = 0, \quad \text{in } \Omega', \tag{3.1a}$$

$$\frac{\partial u}{\partial \mathbf{n}} = g \in H_0^{-1/2}(\Gamma) = \left\{ f : f \in H^{-1/2}(\Gamma), \int_\Gamma f(\mathbf{y})\, dS_\mathbf{y} = 0 \right\}, \tag{3.1b}$$

where g is the given boundary data and $\mathbf{n}$ is the outward normal to the boundary.

A classical way of solving this problem using integral equations consists in using a double layer representation. Thus, we search a density μ defined on Γ such that the solution can be expressed as

$$u(\mathbf{x}) = -\frac{1}{2\pi}\int_{\Gamma}\mu(\mathbf{y})\frac{\partial}{\partial \mathbf{n}_{\mathbf{y}}}\ln|\mathbf{x}-\mathbf{y}|\,dS_{\mathbf{y}} + C^*, \quad \mathbf{x}\in\Omega', \tag{3.2}$$

in which μ is the jump through Γ of the function u, and C^* is a constant. On satisfying the boundary condition in (3.1), we get the following BIE:

$$-\frac{1}{2\pi}\int_{\Gamma}\mu(\mathbf{y})\frac{\partial^2}{\partial \mathbf{n}_{\mathbf{x}}\partial \mathbf{n}_{\mathbf{y}}}\ln|\mathbf{x}-\mathbf{y}|\,dS_{\mathbf{y}} = g(\mathbf{x}), \quad \mathbf{x}\in\Gamma. \tag{3.3}$$

Theorem 3.1. ([20–22]) *The BIE* (3.3) *defines an isomorphism from* $H^{1/2}(\Gamma)\big/\mathbb{R}$ *onto* $H_0^{-1/2}(\Gamma)$ *and equivalent to the following variational problem:*

$$\begin{aligned} &\textit{Find} \quad \mu\in H^{1/2}(\Gamma)\Big/\mathbb{R} \quad \textit{such that} \quad \forall\mu'\in H^{1/2}(\Gamma)\Big/\mathbb{R},\\ &b(\mu,\mu') = \int_{\Gamma} g(\mathbf{y})\,\mu'(\mathbf{y})\,dS_{\mathbf{y}}, \end{aligned} \tag{3.4}$$

where the bilinear form $b(\cdot,\cdot)$ *is symmetric, continuous and coercive on* $H^{1/2}(\Gamma)\big/\mathbb{R}$*, and can be expressed as*

$$b(\mu,\mu') = -\frac{1}{4\pi}\int_{\Gamma}\int_{\Gamma}(\mu(\mathbf{x})-\mu(\mathbf{y}))(\mu'(\mathbf{x})-\mu'(\mathbf{y}))\frac{\partial^2}{\partial \mathbf{n}_{\mathbf{y}}\partial \mathbf{n}_{\mathbf{x}}}\ln|\mathbf{x}-\mathbf{y}|\,dS_{\mathbf{x}}dS_{\mathbf{y}}. \tag{3.5}$$

In the variational problem (3.4), there have integrations over the boundary. In the GBNM, a cell structure is employed to approximate the boundary and carry out numerical integration by Gaussian quadrature while the unknown function μ is approximated by the MLS scheme that only use the boundary nodes. As a result, the boundary and the unknown function are approximated in totally different ways.

3.2. Construction of the integration background cells Γ_h

In this subsection, we will construct an approximate boundary Γ_h as the integration background cells. We choose N_C boundary points A_i such that $A_i = X(\tilde{s}_i)$, $1\le i\le N_C$. Here $\tilde{s}_i$ is the local coordinate of A_i on Γ. We emphasize here that the points A_i are used just for construction of Γ_h, and they are independent of the boundary nodes $\mathbf{x}_i$. We denote

$$\tilde{h} := \max_{1\le i\le N_C}(\tilde{s}_i - \tilde{s}_{i-1}) \quad \text{and} \quad \tilde{h}_i := \left|\overrightarrow{A_{i-1}A_i}\right| = |X(\tilde{s}_i) - X(\tilde{s}_{i-1})|$$

with $\tilde{s}_0 = \tilde{s}_{N_C} - L$, then from the fact that $X(s)$ is continuously differentiable we obtain $\tilde{h}_i = \mathcal{O}(\tilde{h})$. For each integer $i\in[1,N_C]$, we establish a orthogonal local coordinates $(\mathbf{u}_i,\mathbf{v}_i)$ as the following: suppose that the source point is A_{i-1}, and the abscissa axis coincides with the vector $\overrightarrow{A_{i-1}A_i}$. We use Γ_i to denote the curve $A_{i-1}A_i$, then $\Gamma = \bigcup_{i=1}^{N_C}\Gamma_i$, and Γ_i can be represented as

$$\mathbf{x} := \psi_i(\xi) = \left(\xi\tilde{h}_i, f_i(\xi)\right), \quad \xi\in[0,1], \tag{3.6}$$

where

$$f_i(\xi) := \mathbf{v}_i\cdot\overrightarrow{A_{i-1}X(s)}. \tag{3.7}$$

Assume that β is a positive integer. Let $p_i(\xi)$ be the β-degree interpolation of $f_i(\xi)$ on interpolation nodes j/β, $0 \le j \le \beta$, then the approximate curve Γ_{ih} is given by

$$\mathbf{x}_h := \psi_{ih}(\xi) = \left(\xi\tilde{h}_i, p_i(\xi)\right), \quad \xi \in [0,1]. \tag{3.8}$$

In what follows, we shall use $\Gamma_h := \bigcup_{i=1}^{N_C} \Gamma_{ih}$ as the approximate boundary of Γ. Besides, we define the following mapping of Γ onto Γ_h,

$$\Psi := \psi_{ih} \circ \psi_i^{-1}. \tag{3.9}$$

For Γ_h sufficiently close to Γ, i.e., for $\tilde{h}$ sufficiently small, Ψ is regular and bijective.

The curve Γ_h is the background cells, which is an approximation of the boundary Γ. If Γ is a polygonal curve, then Γ_h and Γ can be coincided with each other. In meshless methods, the number of nodes corresponding to each cell is arbitrary. Nonetheless, in order to carry out accurate integration by Gaussian quadrature, it is recommended to use a small number of nodes per cell [8,17,18]. Therefore, we assume that the following assumption is satisfied.

Assumption 3.1. *There exists a nonnegative integer $\bar{K}$ such that there are at most $\bar{K}$ boundary nodes corresponding to each cell.*

In the GBNM, the boundary nodes $\mathbf{x}_i$ are lie on the boundary Γ and are independent of the cells Γ_h. While in the BEM, the boundary nodes are tightly coupled to the boundary element, thus the concept of a cell is quite different from that of an element. Since from (3.9) we deduce $\mathbf{x}_i \circ \Psi \in \Gamma_h$, Assumption 3.1 implies that each cell contains less than $\bar{K}$ points $\mathbf{x}_i \circ \Psi$. Besides, according to Assumption 3.1, the length of each cell can be measured by the parameter h, i.e., $\tilde{h}_i = \mathcal{O}(h)$ with $1 \le i \le N_C$.

Proposition 3.1. ([21,23]) *Assume that $\beta \le \ell - 2$, then for any $\mathbf{x}, \mathbf{y} \in \Gamma$, we have*

$$C_1 |\Psi(\mathbf{x}) - \Psi(\mathbf{y})| \le |\mathbf{x} - \mathbf{y}| \le C_2 |\Psi(\mathbf{x}) - \Psi(\mathbf{y})|, \tag{3.10}$$

$$\left| |\mathbf{x} - \mathbf{y}|^2 - |\Psi(\mathbf{x}) - \Psi(\mathbf{y})|^2 \right| \le C h^{\beta+1} |\mathbf{x} - \mathbf{y}|^2, \tag{3.11}$$

$$|1 - J(\partial\Psi)(\mathbf{x})| \le C h^{\beta+1}, \tag{3.12}$$

where C_1, C_2 and C are constants independent of h, and J denotes the Jacobian,

$$J(\partial\Psi)(\mathbf{x}) := \left|\frac{\partial\psi_{ih}(\xi)}{\partial\xi}\right| \Big/ \left|\frac{\partial\psi_i(\xi)}{\partial\xi}\right|. \tag{3.13}$$

3.3. Construction of an approximate space $V_h(\Gamma_h)$

We define the approximate space as

$$V_h(\Gamma_h) := \operatorname{span}\{\Phi_{ih}, 1 \le i \le N\}, \tag{3.14}$$

where the basis functions Φ_{ih} are defined on the integration background cells Γ_h,

$$\Phi_{ih} := \Phi_i \circ \Psi. \tag{3.15}$$

Here Φ_i is the MLS shape function given in (2.4), and is defined on the boundary Γ.

From (3.9) it follows that the continuous order of the mapping Ψ is β. Then according to Proposition 2.2, we have

Proposition 3.2. *For any* $\mathbf{x} \in \Gamma_h$ *and* $1 \leq i \leq N$, $\Phi_{ih}(\mathbf{x}) \in C_0^{\bar{\gamma}}\left(\Re_h^i\right)$, *where* $\bar{\gamma} := \min(\gamma, \beta)$ *and*

$$\Re_h^i := \Re^i \circ \Psi \subset \Gamma_h. \tag{3.16}$$

Since $V_h(\Gamma_h)$ is not included in $H^{1/2}(\Gamma)$ but in $L^2(\Gamma_h)$, we let $\tilde{V}_h(\Gamma)$ be the subspace of $H^{1/2}(\Gamma)$, the image of $V_h(\Gamma_h)$ by the inverse mapping Ψ^{-1}, i.e.,

$$\tilde{V}_h(\Gamma) := \operatorname{span}\{\Phi_i, 1 \leq i \leq N\}. \tag{3.17}$$

From Proposition 3.2 it follows that $\Phi_{ih} \in C^{\bar{\gamma}}(\Gamma_h)$, $\mathbf{x} \in \Gamma_h$, $1 \leq i \leq N$, thus $\tilde{v}_h \in H^m(\Gamma) \subset H^{1/2}(\Gamma)$ provided that $\tilde{v}_h \in \tilde{V}_h(\Gamma)$ and $1/2 \leq m \leq \bar{\gamma}$.

3.4. The approximate problem

On $V_h(\Gamma_h)$, the variational problem (3.4) can be approximated by

$$\begin{aligned} &\text{Find} \quad \mu_h \in V_h(\Gamma_h)/\mathbb{R} \text{ such that } \forall \mu_h' \in V_h(\Gamma_h)/\mathbb{R}, \\ &b_h(\mu_h, \mu_h') = \int_{\Gamma_h} g_h(\mathbf{y})\, \mu_h'(\mathbf{y})\, dS_{h\mathbf{y}}, \end{aligned} \tag{3.18}$$

where $g_h(\mathbf{y})$ is an approximation of $g(\mathbf{y})$ restricted on Γ_h and satisfying $\int_{\Gamma_h} g_h(\mathbf{y})\, dS_{h\mathbf{y}} = 0$, and

$$\begin{aligned} &b_h(\mu_h, \mu_h') \\ &= -\frac{1}{4\pi} \int_{\Gamma_h} \int_{\Gamma_h} \Big(\mu_h(\mathbf{x}) - \mu_h(\mathbf{y})\Big)\Big(\mu_h'(\mathbf{x}) - \mu_h'(\mathbf{y})\Big) \frac{\partial^2}{\partial \mathbf{n}_{h\mathbf{y}} \partial \mathbf{n}_{h\mathbf{x}}} \ln|\mathbf{x} - \mathbf{y}|\, dS_{h\mathbf{x}} dS_{h\mathbf{y}}. \end{aligned} \tag{3.19}$$

Here $\mathbf{n}_h$ is a β-degree interpolation of $\mathbf{n}$.

Now, we need to show the variational problem (3.18) admits only one solution. In order to do so, we first prove the following lemma.

Lemma 3.1. *There exists a constant* C *independent of* h *such that*

$$\begin{aligned} &|b(\tilde{\mu}_h, \tilde{\mu}_h') - b_h(\mu_h, \mu_h')| \\ &\leq C h^{\beta+1} \|\tilde{\mu}_h\|_{H^{1/2}(\Gamma)/\mathbb{R}} \|\tilde{\mu}_h'\|_{H^{1/2}(\Gamma)/\mathbb{R}}, \qquad \forall \mu_h, \mu_h' \in V_h(\Gamma_h)/\mathbb{R}, \end{aligned} \tag{3.20}$$

where $\tilde{\mu}_h = \mu_h \circ \Psi^{-1} \in \tilde{V}_h(\Gamma)\Big/\mathbb{R}$ *and* $\tilde{\mu}_h' = \mu_h' \circ \Psi^{-1} \in \tilde{V}_h(\Gamma)\Big/\mathbb{R}$.

Proof. We change the integrals in (3.19) into integrals on Γ by the mapping Ψ,

$$\begin{aligned} b_h(\mu_h, \mu_h') = &-\frac{1}{4\pi} \int_{\Gamma} \int_{\Gamma} \Big(\tilde{\mu}_h(\mathbf{x}) - \tilde{\mu}_h(\mathbf{y})\Big)\Big(\tilde{\mu}_h'(\mathbf{x}) - \tilde{\mu}_h'(\mathbf{y})\Big) \\ &\times \frac{\partial^2}{\partial \mathbf{n}_{h\mathbf{y}} \partial \mathbf{n}_{h\mathbf{x}}} \ln\big|\Psi(\mathbf{x}) - \Psi(\mathbf{y})\big| \cdot J(\partial\Psi)(\mathbf{x})\, J(\partial\Psi)(\mathbf{y})\, dS_{\mathbf{x}} dS_{\mathbf{y}}. \end{aligned}$$

Then using (3.5) yields

$$b(\tilde{\mu}_h, \tilde{\mu}_h') - b_h(\mu_h, \mu_h') = R_1 + R_2,$$

where

$$\begin{aligned}R_1 =& -\frac{1}{4\pi}\int_\Gamma\int_\Gamma \Big(\tilde{\mu}_h(\mathbf{x})-\tilde{\mu}_h(\mathbf{y})\Big)\Big(\tilde{\mu}'_h(\mathbf{x})-\tilde{\mu}'_h(\mathbf{y})\Big)\\ &\times\frac{\partial^2}{\partial\mathbf{n_y}\partial\mathbf{n_x}}\ln|\mathbf{x}-\mathbf{y}|\cdot\Big(1-J\left(\partial\Psi\right)(\mathbf{x})\cdot J\left(\partial\Psi\right)(\mathbf{y})\Big)dS_{\mathbf{x}}dS_{\mathbf{y}},\\ R_2 =& -\frac{1}{4\pi}\int_\Gamma\int_\Gamma \Big(\tilde{\mu}_h(\mathbf{x})-\tilde{\mu}_h(\mathbf{y})\Big)\Big(\tilde{\mu}'_h(\mathbf{x})-\tilde{\mu}'_h(\mathbf{y})\Big)\\ &\times\left(\frac{\partial^2}{\partial\mathbf{n_y}\partial\mathbf{n_x}}\ln|\mathbf{x}-\mathbf{y}|-\frac{\partial^2}{\partial\mathbf{n}_{h\mathbf{y}}\partial\mathbf{n}_{h\mathbf{x}}}\ln\left|\Psi\left(\mathbf{x}\right)-\Psi\left(\mathbf{y}\right)\right|\right)J\left(\partial\Psi\right)(\mathbf{x})\,J\left(\partial\Psi\right)(\mathbf{y})\,dS_{\mathbf{x}}dS_{\mathbf{y}}.\end{aligned}$$

According to (3.12), one gets

$$\left|J\left(\partial\Psi\right)(\mathbf{x})\right|\le C, \tag{3.21}$$

and

$$\begin{aligned}&\left|1-J\left(\partial\Psi\right)(\mathbf{x})\cdot J\left(\partial\Psi\right)(\mathbf{y})\right|\\ \le&\left|1-J\left(\partial\Psi\right)(\mathbf{x})\right|+\left|J\left(\partial\Psi\right)(\mathbf{x})\right|\cdot\left|1-J\left(\partial\Psi\right)(\mathbf{y})\right|\le Ch^{\beta+1}.\end{aligned}$$

Thus using the continuity of $b\left(\cdot,\cdot\right)$ yields

$$|R_1|\le Ch^{\beta+1}\left\|\tilde{\mu}_h\right\|_{H^{1/2}(\Gamma)/\mathbb{R}}\left\|\tilde{\mu}'_h\right\|_{H^{1/2}(\Gamma)/\mathbb{R}}.$$

On the other hand, from the fact that $\mathbf{n}_h$ is the β-th interpolation of $\mathbf{n}$ we have

$$|\mathbf{n_x}-\mathbf{n}_{h\mathbf{x}}|\le Ch^{\beta+1}. \tag{3.22}$$

Then, the terms $\left(\mathbf{n_x}-\mathbf{n}_{h\mathbf{x}},\mathbf{n_x}\right)|\mathbf{x}-\mathbf{y}|^{-2}$ and $\left(\mathbf{x}-\mathbf{y},\mathbf{n_x}-\mathbf{n}_{h\mathbf{x}}\right)\left(\mathbf{x}-\mathbf{y},\mathbf{n_y}\right)|\mathbf{x}-\mathbf{y}|^{-4}$ can be bounded above by $Ch^{\beta+1}|\mathbf{x}-\mathbf{y}|^{-2}$. Moreover, using Proposition 3.1, the bounds for the three terms

$$|\mathbf{x}-\mathbf{y}|^{-2}-\big|\Psi(\mathbf{x})-\Psi(\mathbf{y})\big|^{-2},\qquad\big(\mathbf{x}-\mathbf{y},\mathbf{n}_{h\mathbf{x}}\big)\big(\mathbf{x}-\mathbf{y}-\Psi(\mathbf{x})+\Psi(\mathbf{y}),\mathbf{n_x}\big)|\mathbf{x}-\mathbf{y}|^{-4},$$

and

$$\Big(\Psi\left(\mathbf{x}\right)-\Psi\left(\mathbf{y}\right),\mathbf{n}_{h\mathbf{x}}\Big)\Big(\Psi\left(\mathbf{x}\right)-\Psi\left(\mathbf{y}\right),\mathbf{n}_{h\mathbf{y}}\Big)\left(|\mathbf{x}-\mathbf{y}|^{-4}-|\Psi\left(\mathbf{x}\right)-\Psi\left(\mathbf{y}\right)|^{-4}\right),$$

are $Ch^{\beta+1}|\mathbf{x}-\mathbf{y}|^{-2}$. As a result, we obtain

$$\begin{aligned}&\frac{\partial^2}{\partial\mathbf{n_y}\partial\mathbf{n_x}}\ln|\mathbf{x}-\mathbf{y}|-\frac{\partial^2}{\partial\mathbf{n}_{h\mathbf{y}}\partial\mathbf{n}_{h\mathbf{x}}}\ln\left|\Psi\left(\mathbf{x}\right)-\Psi\left(\mathbf{y}\right)\right|\\ =&-\frac{\left(\mathbf{n_x},\mathbf{n_y}\right)}{\left|\mathbf{x}-\mathbf{y}\right|^2}+\frac{\left(\mathbf{n}_{h\mathbf{x}},\mathbf{n}_{h\mathbf{y}}\right)}{\left|\Psi\left(\mathbf{x}\right)-\Psi\left(\mathbf{y}\right)\right|^2}+\frac{2\left(\mathbf{x}-\mathbf{y},\mathbf{n_x}\right)\left(\mathbf{x}-\mathbf{y},\mathbf{n_y}\right)}{\left|\mathbf{x}-\mathbf{y}\right|^4}\\ &-\frac{2\big(\Psi\left(\mathbf{x}\right)-\Psi\left(\mathbf{y}\right),\mathbf{n}_{h\mathbf{x}}\big)\left(\Psi\left(\mathbf{x}\right)-\Psi\left(\mathbf{y}\right),\mathbf{n}_{h\mathbf{y}}\right)}{\left|\Psi\left(\mathbf{x}\right)-\Psi\left(\mathbf{y}\right)\right|^4}\\ \le&Ch^{\beta+1}\left|\mathbf{x}-\mathbf{y}\right|^{-2}.\end{aligned}$$

Therefore

$$|R_2|\le Ch^{\beta+1}\int_\Gamma\int_\Gamma\Big(\tilde{\mu}_h\left(\mathbf{x}\right)-\tilde{\mu}_h\left(\mathbf{y}\right)\Big)\Big(\tilde{\mu}'_h\left(\mathbf{x}\right)-\tilde{\mu}'_h\left(\mathbf{y}\right)\Big)\left|\mathbf{x}-\mathbf{y}\right|^{-2}dS_{\mathbf{x}}dS_{\mathbf{y}}.$$

As in the 3-D case [20, 21], we can verify that

$$b(\mu) := \left(\int_\Gamma \int_\Gamma \left(\mu(\mathbf{x}) - \mu(\mathbf{y}) \right)^2 |\mathbf{x} - \mathbf{y}|^{-2} \, dS_{\mathbf{x}} dS_{\mathbf{y}} \right)^{\frac{1}{2}}$$

is a norm on $H^{1/2}(\Gamma)/\mathbb{R}$ equivalent to the usual norm. Thus the proof is complete. □

Theorem 3.2. *The variational problem* (3.18) *has one and only one solution.*

Proof. By using Lemma 3.1, we have

$$b_h(\mu_h, \mu_h) \geq b(\tilde{\mu}_h, \tilde{\mu}_h) - Ch^{\beta+1} \|\tilde{\mu}_h\|^2_{H^{1/2}(\Gamma)/\mathbb{R}}, \quad \tilde{\mu}_h = \mu_h \circ \Psi.$$

Since $\tilde{\mu}_h \in \tilde{V}_h(\Gamma)\big/\mathbb{R} \subset H^{1/2}(\Gamma)/\mathbb{R}$ and $b(\cdot,\cdot)$ is coercive on $H^{1/2}(\Gamma)/\mathbb{R}$, one gets

$$b(\tilde{\mu}_h, \tilde{\mu}_h) \geq C_1 \|\tilde{\mu}_h\|^2_{H^{1/2}(\Gamma)/\mathbb{R}}, \quad C_1 > 0.$$

Then, for h sufficiently small, there exists a constant $C' > 0$ such that

$$b_h(\mu_h, \mu_h) \geq C_1 \|\tilde{\mu}_h\|^2_{H^{1/2}(\Gamma)/\mathbb{R}} - Ch^{\beta+1} \|\tilde{\mu}_h\|^2_{H^{1/2}(\Gamma)/\mathbb{R}} \geq C' \|\tilde{\mu}_h\|^2_{H^{1/2}(\Gamma)/\mathbb{R}}. \tag{3.23}$$

Thus the bilinear form $b_h(\cdot,\cdot)$ is positive definite on $V_h(\Gamma_h)/\mathbb{R}$. Besides, we can easily verify that $b_h(\cdot,\cdot)$ is symmetric and $\int_{\Gamma_h} g_h(\mathbf{y}) \mu'_h(\mathbf{y}) \, dS_{h\mathbf{y}}$ is a continuous linear functional on $V_h(\Gamma_h)/\mathbb{R}$. As a result, the Lax-Milgram theorem is applied, and we conclude that the variational problem (3.18) has a unique solution $\mu_h \in V_h(\Gamma_h)/\mathbb{R}$. □

On $V_h(\Gamma_h)/\mathbb{R}$, the Galerkin approximation μ_h of the real solution μ may be written as

$$\mu_h(\mathbf{x}) = \sum_{i \in \wedge(\mathbf{x})} \Phi_{ih}(\mathbf{x}) \mu_i. \tag{3.24}$$

Substituting (3.24) into (3.18), by virtue of Proposition 3.2, one gets the linear system

$$\sum_{i=1}^{N} a_{ij} \mu_i = f_j, \quad 1 \leq j \leq N, \tag{3.25}$$

where

$$a_{ij} = -\frac{1}{4\pi} \int_{\Re_h^j} \int_{\Re_h^i} \left(\Phi_{ih}(\mathbf{x}) - \Phi_{ih}(\mathbf{y}) \right) \left(\Phi_{jh}(\mathbf{x}) - \Phi_{jh}(\mathbf{y}) \right) \times \frac{\partial^2}{\partial \mathbf{n}_{h\mathbf{y}} \partial \mathbf{n}_{h\mathbf{x}}} \ln |\mathbf{x} - \mathbf{y}| \, dS_{h\mathbf{x}} dS_{h\mathbf{y}}, \tag{3.26}$$

$$f_j = \int_{\Re_h^j} g_h(\mathbf{y}) \Phi_{jh}(\mathbf{y}) \, dS_{h\mathbf{y}}, \tag{3.27}$$

where $\Re_h^j$ and $\Re_h^i$ are defined by (3.16), and are parts of the integration background cells Γ_h.

Remark 3.1. From the above development, one can see that the integration cells Γ_h is used for integration only, and Γ_h is not employed in the boundary variable approximation. Besides, there is no relationship between Γ_h and the boundary nodes. Thus, the role of integration cells in the GBNM is different from that of elements in the BEM.

Remark 3.2. The boundary function is multiplied by the MLS shape function and integrated over the boundary. Therefore, boundary conditions can be satisfied directly despite the MLS shape functions lack the property of a delta function.

Remark 3.3. The system matrix $[a_{ij}]$ in (3.25) is symmetric.

Once μ_i are found from the linear system (3.25), the approximate solution u_h of problem (3.1) can be calculated from an approximation form of the formula (3.2)

$$\begin{aligned} u_h(\mathbf{x}) &= -\frac{1}{2\pi}\int_{\Gamma_h}\mu_h(\mathbf{y})\frac{\partial}{\partial \mathbf{n_y}}\ln|\mathbf{x}-\mathbf{y}|\,dS_{h\mathbf{y}} + C^* \\ &= -\frac{1}{2\pi}\sum_{i=1}^{N}\mu_i\int_{\Re_h^i}\Phi_{ih}(\mathbf{y})\frac{\partial}{\partial \mathbf{n_y}}\ln|\mathbf{x}-\mathbf{y}|\,dS_{h\mathbf{y}} + C^*, \quad \mathbf{x}\in\Omega'. \end{aligned} \tag{3.28}$$

4. Error Estimates

In this section, we will prove that the result obtained using the GBNM converges to the solution of problem (3.1) gradually. In order to obtain our main theorems regarding the error estimates for solving problem (3.1), we need first to prove the following theorem which gives the convergence of the solution of the approximate variational problem (3.18) to the exact solution of the variational problem (3.4).

Theorem 4.1. *Let $\mu(\mathbf{x})$ and $\mu_h(\mathbf{x})$ be the solutions of variational problems* (3.4) *and* (3.18)*, respectively. Let us assume that $\tilde{\mu}_h := \mu_h\circ\Psi^{-1}\in\tilde{V}_h(\Gamma)$, then if $\mu(\mathbf{x})\in H^{m+1}(\Gamma)/\mathbb{R}$ with $1/2\le m\le\bar{\gamma}$, we have*

$$\begin{aligned} &\|\mu-\tilde{\mu}_h\|_{H^{1/2}(\Gamma)/\mathbb{R}} \\ &\le C\left\{\|g-\hat{g}_h\|_{H_0^{-1/2}(\Gamma)} + h^{m+3/2}\|\mu\|_{H^{m+1}(\Gamma)/\mathbb{R}} + h^{\beta+1}\|\mu\|_{H^{1/2}(\Gamma)/\mathbb{R}}\right\}, \end{aligned} \tag{4.1}$$

$$\begin{aligned} &\|\mu-\tilde{\mu}_h\|_{H^{-k}(\Gamma)/\mathrm{R}} \\ &\le C\Big\{h^{k+1/2}\|g-\hat{g}_h\|_{H_0^{-1/2}(\Gamma)} + \|g-\hat{g}_h\|_{H_0^{-k-1}(\Gamma)} \\ &\qquad + h^{m+k+1}\|\mu\|_{H^{m+1}(\Gamma)/\mathbb{R}} + h^{\beta+1}\|\mu\|_{H^{1/2}(\Gamma)/\mathbb{R}}\Big\}, \end{aligned} \tag{4.2}$$

where $-1/2\le k\le\gamma$, C is a constant independent of h, and

$$\hat{g}_h(\mathbf{x}) = \left(g_h\circ\Psi^{-1}\right)(\mathbf{x})\cdot J(\partial\Psi)(\mathbf{x}).$$

Proof. Since $\mathcal{M}\mu\in\tilde{V}_h(\Gamma)\Big/\mathbb{R}$ and $\mathcal{M}\mu\circ\Psi\in V_h(\Gamma_h)/\mathbb{R}$, we have

$$\begin{aligned} b_h\big(\mu_h-\mathcal{M}\mu\circ\Psi,\mu_h-\mathcal{M}\mu\circ\Psi\big) &= \langle\hat{g}_h-g,\tilde{\mu}_h-\mathcal{M}\mu\rangle_{L^2(\Gamma)} + b\big(\mu-\mathcal{M}\mu,\tilde{\mu}_h-\mathcal{M}\mu\big) \\ &\quad + b\big(\mathcal{M}\mu,\tilde{\mu}_h-\mathcal{M}\mu\big) - b_h\big(\mathcal{M}\mu\circ\Psi,\mu_h-\mathcal{M}\mu\circ\Psi\big). \end{aligned}$$

Then, according to (3.23), Lemma 3.1 and the continuity of $b(\cdot,\cdot)$, we obtain

$$\begin{aligned} &\|\tilde{\mu}_h-\mathcal{M}\mu\|_{H^{1/2}(\Gamma)/\mathbb{R}} \\ &\le C\left\{\|g-\hat{g}_h\|_{H_0^{-1/2}(\Gamma)} + \|\mu-\mathcal{M}\mu\|_{H^{1/2}(\Gamma)/\mathbb{R}} + h^{\beta+1}\|\mathcal{M}\mu\|_{H^{1/2}(\Gamma)/\mathbb{R}}\right\}. \end{aligned}$$

Thus, using Theorem 2.1 leads to

$$\begin{aligned}
&\|\mu-\tilde{\mu}_h\|_{H^{1/2}(\Gamma)/\mathbb{R}}\\
\leq\ &\|\mu-\mathcal{M}\mu\|_{H^{1/2}(\Gamma)/\mathbb{R}}+\|\mathcal{M}\mu-\tilde{\mu}_h\|_{H^{1/2}(\Gamma)/\mathbb{R}}\\
\leq\ &C\left\{\|g-\hat{g}_h\|_{H_0^{-1/2}(\Gamma)}+\|\mu-\mathcal{M}\mu\|_{H^{1/2}(\Gamma)/\mathbb{R}}+h^{\beta+1}\|\mathcal{M}\mu\|_{H^{1/2}(\Gamma)/\mathbb{R}}\right\}\\
\leq\ &C\left\{\|g-\hat{g}_h\|_{H_0^{-1/2}(\Gamma)}+h^{m+3/2}\|\mu\|_{H^{m+1}(\Gamma)/\mathbb{R}}+h^{\beta+1}\|\mu\|_{H^{1/2}(\Gamma)/\mathbb{R}}\right\}. \qquad (4.3)
\end{aligned}$$

Let $\omega\in H^{\gamma+1}(\Gamma)/\mathbb{R}$ be the solution of

$$\bar{g}(\mathbf{x})=-\frac{1}{2\pi}\int_\Gamma\omega(\mathbf{y})\frac{\partial^2}{\partial\mathbf{n}_\mathbf{x}\partial\mathbf{n}_\mathbf{y}}\ln|\mathbf{x}-\mathbf{y}|\,dS_\mathbf{y}+C^*,\quad \mathbf{x}\in\Gamma. \qquad (4.4)$$

Then according to Theorem 3.1,

$$\|\omega\|_{H^{\gamma+1}(\Gamma)/\mathbb{R}}\leq C\|\bar{g}\|_{H_0^\gamma(\Gamma)}.$$

Thus by the duality argument, we obtain

$$\|\mu-\tilde{\mu}_h\|_{H^{-\gamma}(\Gamma)/\mathbb{R}}=\sup_{\bar{g}\in H_0^\gamma(\Gamma)}\frac{\langle\mu-\tilde{\mu}_h,\bar{g}\rangle_{L^2(\Gamma)}}{\|\bar{g}\|_{H_0^\gamma(\Gamma)}}\leq C\sup_{\omega\in H^{\gamma+1}(\Gamma)/\mathbb{R}}\frac{b(\mu-\tilde{\mu}_h,\omega)}{\|\omega\|_{H^{\gamma+1}(\Gamma)/\mathbb{R}}}. \qquad (4.5)$$

Now, we have

$$b(\mu-\tilde{\mu}_h,\omega)=b(\mu-\tilde{\mu}_h,\omega-\mathcal{M}\omega)+b(\mu-\tilde{\mu}_h,\mathcal{M}\omega). \qquad (4.6)$$

Applying (4.3) and Theorem 2.1, we get

$$\begin{aligned}
&b(\mu-\tilde{\mu}_h,\omega-\mathcal{M}\omega)\\
\leq\ &C\|\mu-\tilde{\mu}_h\|_{H^{1/2}(\Gamma)/\mathbb{R}}\|\omega-\mathcal{M}\omega\|_{H^{1/2}(\Gamma)/\mathbb{R}} \qquad (4.7)\\
\leq\ &Ch^{\gamma+1/2}\left\{\|g-\hat{g}_h\|_{H_0^{-1/2}(\Gamma)}+h^{m+3/2}\|\mu\|_{H^{m+1}(\Gamma)/\mathbb{R}}+h^{\beta+1}\|\mu\|_{H^{1/2}(\Gamma)/\mathbb{R}}\right\}\|\omega\|_{H^{\gamma+1}(\Gamma)/\mathbb{R}}.
\end{aligned}$$

Besides, according to Lemma 3.1, we obtain

$$\begin{aligned}
b(\mu-\tilde{\mu}_h,\mathcal{M}\omega)&=b(\mu,\mathcal{M}\omega)-b(\tilde{\mu}_h,\mathcal{M}\omega)\\
&=\langle g,\mathcal{M}\omega\rangle_{L^2(\Gamma)}-\langle\hat{g}_h,\mathcal{M}\omega\rangle_{L^2(\Gamma)}+b_h(\mu_h,\mathcal{M}\omega\circ\Psi)-b(\tilde{\mu}_h,\mathcal{M}\omega)\\
&\leq C\|g-\hat{g}_h\|_{H_0^{-\gamma-1}(\Gamma)}\|\mathcal{M}\omega\|_{H^{\gamma+1}(\Gamma)/\mathbb{R}}+Ch^{\beta+1}\|\tilde{\mu}_h\|_{H^{1/2}(\Gamma)/\mathbb{R}}\|\mathcal{M}\omega\|_{H^{1/2}(\Gamma)/\mathbb{R}}\\
&\leq C\left\{\|g-\hat{g}_h\|_{H_0^{-\gamma-1}(\Gamma)}+h^{\beta+1}\|\mu\|_{H^{1/2}(\Gamma)/\mathbb{R}}\right\}\|\omega\|_{H^{\gamma+1}(\Gamma)/\mathbb{R}}. \qquad (4.8)
\end{aligned}$$

By gathering (4.5)-(4.8) we can prove (4.2) for $k=\gamma$. For the remaining case $-1/2<k<\gamma$, an interpolation [19] between the already obtained inequalities yields (4.2). □

Theorem 4.2. *Let $u(\mathbf{x})$ be given by (3.2) satisfying $\int_\Gamma\mu(\mathbf{y})\,dS_\mathbf{y}=0$, and let $u_h(\mathbf{x})$ be given by (3.28) satisfying $\int_{\Gamma_h}\mu_h(\mathbf{y})\,dS_{h\mathbf{y}}=0$. Suppose that $\mu(\mathbf{x})\in H^{m+1}(\Gamma)/\mathbb{R}$ with $1/2\leq m\leq\bar{\gamma}$. Then there exists a constant $\delta>0$, for any $\mathbf{x}\in\Omega'$ with $d_\mathbf{x}:=\min_{\mathbf{y}\in\Gamma}|\mathbf{x}-\mathbf{y}|\geq\delta$ and h small enough, we have a constant C independent of h such that*

$$\begin{aligned}
\left|\partial^\lambda u(\mathbf{x})-\partial^\lambda u_h(\mathbf{x})\right|\leq&C\sum_{j=0}^{\gamma}(d_\mathbf{x})^{-j-|\lambda|-1}\left\{h^{\gamma+1/2}\|g-\hat{g}_h\|_{H_0^{-1/2}(\Gamma)}+\|g-\hat{g}_h\|_{H_0^{-\gamma-1}(\Gamma)}\right.\\
&\left.+h^{m+\gamma+1}\|\mu\|_{H^{m+1}(\Gamma)/\mathrm{R}}+h^{\beta+1}\|\mu\|_{H^{1/2}(\Gamma)}\right\},\qquad |\lambda|\geq 0. \qquad (4.9)
\end{aligned}$$

Proof. We change the expression of u_h by the application of Ψ, then

$$\begin{aligned} & u(\mathbf{x}) - u_h(\mathbf{x}) \\ = & -\frac{1}{2\pi}\int_\Gamma \left(\mu(\mathbf{y})\frac{\partial}{\partial \mathbf{n_y}}\ln|\mathbf{x}-\mathbf{y}| - \tilde{\mu}_h(\mathbf{y})\frac{\partial}{\partial \mathbf{n_y}}\ln|\mathbf{x}-\Psi(\mathbf{y})|\cdot J(\partial\Psi)(\mathbf{y})\right) dS_{\mathbf{y}} \\ = & M_1 + M_2, \end{aligned} \tag{4.10}$$

where

$$\begin{aligned} M_1 &= -\frac{1}{2\pi}\int_\Gamma \left(\mu(\mathbf{y}) - \tilde{\mu}_h(\mathbf{y})\cdot J(\partial\Psi)(\mathbf{y})\right)\frac{\partial}{\partial \mathbf{n_y}}\ln|\mathbf{x}-\mathbf{y}|\, dS_{\mathbf{y}}, \\ M_2 &= -\frac{1}{2\pi}\int_\Gamma \tilde{\mu}_h(\mathbf{y})\cdot J(\partial\Psi)(\mathbf{y})\left(\frac{\partial}{\partial \mathbf{n_y}}\ln|\mathbf{x}-\mathbf{y}| - \frac{\partial}{\partial \mathbf{n_y}}\ln|\mathbf{x}-\Psi(\mathbf{y})|\right) dS_{\mathbf{y}}. \end{aligned}$$

Since $d_{\mathbf{x}} \geq \delta$, we have

$$\left\|\frac{\partial}{\partial \mathbf{n_y}}\ln|\mathbf{x}-\mathbf{y}|\right\|_{H^\gamma(\Gamma)} = \left\|\frac{\cos(\mathbf{y}-\mathbf{x},\mathbf{n_y})}{|\mathbf{x}-\mathbf{y}|}\right\|_{H^\gamma(\Gamma)} \leq C\sum_{j=0}^{\gamma}(d_{\mathbf{x}})^{-j-1}.$$

Note that

$$\|\mu - \tilde{\mu}_h\cdot J(\partial\Psi)\|_{H^{-\gamma}(\Gamma)/\mathbb{R}} \leq \|\mu-\tilde{\mu}_h\|_{H^{-\gamma}(\Gamma)/\mathbb{R}} + \|\tilde{\mu}_h(1-J(\partial\Psi))\|_{H^{-\gamma}(\Gamma)/\mathbb{R}}.$$

From (3.12) and (4.1) we have

$$\|\tilde{\mu}_h(1-J(\partial\Psi))\|_{H^{-\gamma}(\Gamma)/\mathbb{R}} \leq Ch^{\beta+1}\|\tilde{\mu}_h\|_{H^{1/2}(\Gamma)/\mathbb{R}} \leq Ch^{\beta+1}\|\mu\|_{H^{1/2}(\Gamma)/\mathbb{R}}.$$

It follows from

$$\int_\Gamma \tilde{\mu}_h J(\partial\Psi)\, dS = \int_{\Gamma_h}\mu_h dS_h = 0 \tag{4.11}$$

that

$$\int_\Gamma \left(\mu(\mathbf{y}) - \tilde{\mu}_h(\mathbf{y})\cdot J(\partial\Psi)(\mathbf{y})\right) dS_{\mathbf{y}} = 0.$$

Hence,

$$\begin{aligned} |M_1| \leq & \|\mu-\tilde{\mu}_h\cdot J(\partial\Psi)\|_{H^{-\gamma}(\Gamma)/\mathbb{R}}\left\|\frac{\partial}{\partial \mathbf{n_y}}\ln|\mathbf{x}-\mathbf{y}|\right\|_{H_0^\gamma(\Gamma)} \\ \leq & C\sum_{j=0}^{\gamma}(d_{\mathbf{x}})^{-j-1}\left(\|\mu-\tilde{\mu}_h\|_{H^{-\gamma}(\Gamma)/\mathbb{R}} + h^{\beta+1}\|\mu\|_{H^{1/2}(\Gamma)/\mathbb{R}}\right). \end{aligned} \tag{4.12}$$

On the other hand, according to Proposition 3.1 and (3.22),

$$\begin{aligned} & \left\|\frac{\partial}{\partial \mathbf{n_y}}\ln|\mathbf{x}-\mathbf{y}| - \frac{\partial}{\partial \mathbf{n_y}}\ln|\mathbf{x}-\Psi(\mathbf{y})|\right\|_{L^2(\Gamma)} = \left\|\frac{(\mathbf{y}-\mathbf{x},\mathbf{n_y})}{|\mathbf{x}-\mathbf{y}|^2} - \frac{(\Psi(\mathbf{y})-\mathbf{x},\mathbf{n}_{h\mathbf{y}})}{|\mathbf{x}-\Psi(\mathbf{y})|^2}\right\|_{L^2(\Gamma)} \\ \leq & \left\|\frac{(\mathbf{y}-\mathbf{x},\mathbf{n_y}) - (\Psi(\mathbf{y})-\mathbf{x},\mathbf{n}_{h\mathbf{y}})}{|\mathbf{x}-\mathbf{y}|^2}\right\|_{L^2(\Gamma)} + \left\|(\Psi(\mathbf{y})-\mathbf{x},\mathbf{n}_{h\mathbf{y}})\left(\frac{1}{|\mathbf{x}-\mathbf{y}|^2} - \frac{1}{|\mathbf{x}-\Psi(\mathbf{y})|^2}\right)\right\|_{L^2(\Gamma)} \\ \leq & Ch^{\beta+1}\sum_{j=0}^{2}(d_{\mathbf{x}})^{-j}. \end{aligned}$$

And applying (4.11) leads to

$$\|\tilde{\mu}_h J(\partial\Psi)\|_{L^2(\Gamma)} = \|\mu_h\|_{L^2(\Gamma_h)/\mathbb{R}} \le C\|\mu\|_{L^2(\Gamma)/\mathbb{R}} \le C\|\mu\|_{H^{1/2}(\Gamma)/\mathbb{R}}.$$

Therefore,

$$\begin{aligned}|M_2| &\le \|\tilde{\mu}_h J(\partial\Psi)\|_{L^2(\Gamma)} \left\| \frac{\partial}{\partial \mathbf{n}_\mathbf{y}} \ln|\mathbf{x}-\mathbf{y}| - \frac{\partial}{\partial \mathbf{n}_\mathbf{y}} \ln|\mathbf{x}-\Psi(\mathbf{y})| \right\|_{L^2(\Gamma)} \\ &\le Ch^{\beta+1} \sum_{j=0}^{2} (d_\mathbf{x})^{-j} \|\mu\|_{H^{1/2}(\Gamma)/\mathbb{R}}. \end{aligned} \tag{4.13}$$

By substituting (4.12) and (4.13) into (4.10) and by using Theorem 4.2 we can prove (4.9) for $|\lambda| = 0$. Other cases are similar. □

Remark 4.1. Contrary to the case of the domain type methods, such as the FEM, Theorem 4.2 indicates that the errors of the potential u and its successive derivatives in the GBNM are all of the same order.

Remark 4.2. If $\mu(\mathbf{x}) \in H^{\gamma+1}(\Gamma)/\mathbb{R}$, we can conclude from Theorems 4.1 and 4.2 that the error on the jump of the solution through Γ is optimal when $\beta = \gamma$, whereas the error on the solution, far enough from Γ, is optimal when $\beta = 2\gamma$. This phenomenon also occurs in the Galerkin BEM for solving 3-D Neumann problems [20, 21].

If the boundary Γ is a polygonal curve, then Γ_h and Γ can be coincided with each other. In this case, the approximate space defined by (3.14) is simplified as

$$V_h(\Gamma) = \operatorname{span}\{\Phi_i, 1 \le i \le N\},$$

and the approximate solution $u_h(\mathbf{x})$ will be determined by

$$\begin{aligned} u_h(\mathbf{x}) &= -\frac{1}{2\pi} \int_\Gamma \mu_h(\mathbf{y}) \frac{\partial}{\partial \mathbf{n}_\mathbf{y}} \ln|\mathbf{x}-\mathbf{y}| \, dS_\mathbf{y} + C^* \\ &= -\frac{1}{2\pi} \sum_{i=1}^{N} \mu_i \int_{\Re^i} \Phi_i(\mathbf{y}) \frac{\partial}{\partial \mathbf{n}_\mathbf{y}} \ln|\mathbf{x}-\mathbf{y}| \, dS_\mathbf{y} + C^*. \end{aligned} \tag{4.14}$$

Now, the results of Theorem 4.2 can be rewritten as

$$\begin{aligned} &\left|\partial^\lambda u(\mathbf{x}) - \partial^\lambda u_h(\mathbf{x})\right| \\ &\le C \sum_{j=0}^{\gamma} (d_\mathbf{x})^{-j-|\lambda|-1} h^{m+\gamma+1} \|\mu\|_{H^{m+1}(\Gamma)/\mathbb{R}}, \qquad |\lambda| \ge 0, \quad 1/2 \le m \le \gamma. \end{aligned} \tag{4.15}$$

Besides, the convergence order of solving the problem (3.1) will be established in energy norms. That is

Theorem 4.3. *Let $u(\mathbf{x})$ and $u_h(\mathbf{x})$ be given by (3.2) and (4.14), respectively. Then if $\mu(\mathbf{x}) \in H^{m+1}(\Gamma)/\mathbb{R}$, there is a constant C independent of h such that*

$$\|u - u_h\|_{W_0^1(\Omega')/\mathbb{R}} \le Ch^{m+1/2} \|\mu\|_{H^{m+1}(\Gamma)/\mathbb{R}}, \qquad 1/2 \le m \le \gamma. \tag{4.16}$$

where $W_0^1(\Omega')$ denotes a weighted Sobolev spaces [20–22].

Proof. If there is no difference between the boundary Γ and the integration background cells Γ_h, the results of Theorem 4.1 shall be simplified as

$$\|\mu-\mu_h\|_{H^{-k}(\Gamma)/\mathbb{R}} \leq Ch^{m+k+1}\|\mu\|_{H^{m+1}(\Gamma)/\mathbb{R}}, \qquad -1/2 \leq k \leq \gamma. \tag{4.17}$$

Consequently, using Theorem 3.1 we have

$$\|u-u_h\|_{W_0^1(\Omega')/\mathbb{R}} \leq C\|\mu-\mu_h\|_{H^{1/2}(\Gamma)/\mathbb{R}} \leq Ch^{m+1/2}\|\mu\|_{H^{m+1}(\Gamma)/\mathbb{R}}.$$

This completes the proof of the theorem. □

5. Numerical Aspects

The evaluation of the coefficient a_{ij} in (3.26) is the most important operation in this approach because it involves a hypersingular kernel. It is difficult to directly get singular integrals of a_{ij}. There are many regularization procedures to reduce hypersingularity are available in the literature [24, 25]. The scheme of integration by parts in the sense of distributions is commonly used to reduce the hypersingularity integral into a weak one, which shifted the partial derivatives of hypersingular kernel to the unknown function in the variational formulation. The approach to shifting the partial derivatives of hypersingular kernel to the boundary rotation (curl) of unknown function in 3-D cases was developed by Nedelec [22, 26]. Recently, Zhu et al. extended this technique to 2-D problems [25].

To any function μ defined on Γ, we associate

$$\overrightarrow{\mathrm{rot}_\Gamma}\mu = \mathrm{grad}\,\mu \times \mathbf{n}. \tag{5.1}$$

Then the bilinear form $b(\cdot,\cdot)$ given by (3.5) has the expression

$$b(\mu,\mu') = \frac{1}{2\pi}\int_\Gamma\int_\Gamma \ln|\mathbf{x}-\mathbf{y}|\,\overrightarrow{\mathrm{rot}_\Gamma}\mu(\mathbf{x})\cdot\overrightarrow{\mathrm{rot}_\Gamma}\mu'(\mathbf{y})\,dS_{\mathbf{x}}dS_{\mathbf{y}}. \tag{5.2}$$

Thus, (3.26) can be rewritten as

$$a_{ij} = b_h(\Phi_{ih},\Phi_{jh}) = \frac{1}{2\pi}\int_{\Re_h^j}\int_{\Re_h^i}\ln|\mathbf{x}-\mathbf{y}|\,\overrightarrow{\mathrm{rot}_{\Gamma_h}}\Phi_{ih}(\mathbf{x})\cdot\overrightarrow{\mathrm{rot}_{\Gamma_h}}\Phi_{jh}(\mathbf{y})\,dS_{h\mathbf{x}}dS_{h\mathbf{y}}. \tag{5.3}$$

For calculating the boundary rotation, a linear geometric representation is applied in this research, i.e. $\beta = 1$. In this case, the cells Γ_{kh}, $1 \leq k \leq N_C$, can be expressed as

$$x_j = x_j^k\phi^1(\xi) + x_j^{k+1}\phi^2(\xi), \qquad \xi \in [-1,1], \quad j = 1,2,$$

where $\left(x_1^k, x_2^k\right)$ and $\left(x_1^{k+1}, x_2^{k+1}\right)$ are the Cartesian co-ordinates of the ends of Γ_{kh}, and $\phi^1(\xi) = 0.5(1-\xi)$, $\phi^2(\xi) = 0.5(1+\xi)$. Clearly, the outward normal to Γ_{kh} is

$$\mathbf{n}(\mathbf{x}) = \left(\frac{x_2^{k+1}-x_2^k}{l_k}, -\frac{x_1^{k+1}-x_1^k}{l_k}\right)$$

with l_k is the length of Γ_{kh}. Let $\mathbf{i}$ and $\mathbf{j}$ denote the coordinate axis on the plan and $\mathbf{k} = \mathbf{i}\times\mathbf{j}$. Then from (5.1) we have

$$\begin{aligned}\overrightarrow{\mathrm{rot}_{\Gamma_h}}\Phi_{ih}(\mathbf{x}) &= \mathrm{grad}\,\Phi_{ih}(\mathbf{x})\times\mathbf{n}(\mathbf{x})\\ &= -\left(\frac{x_1^{k+1}-x_1^k}{l_k}\frac{\partial\Phi_{ih}(\mathbf{x})}{\partial x_1} + \frac{x_2^{k+1}-x_2^k}{l_k}\frac{\partial\Phi_{ih}(\mathbf{x})}{\partial x_2}\right)\mathbf{k}.\end{aligned} \tag{5.4}$$

Substituting (5.4) into (5.3), the integrations involves only logarithmical singular functions that can be calculated by logarithmical Gaussian quadrature.

6. Numerical Experiments

In this section, we will present numerical results on theoretical results of the GBNM. In all examples, the polynomial basis is chosen as a quadratic basis, that is $\bar{\mathfrak{m}} = 2$ in (2.4). Besides, the weight function is chosen as the following spline,

$$w(d) = \begin{cases} 1 - 6d^2 + 8d^3 - 3d^4, & d \le 1, \\ 0, & d > 1, \end{cases}$$

where $d = |\mathbf{x} - \mathbf{x}_i|/\bar{d}$, $\bar{d}$ is the radius of the influence domain of boundary points. In computations, $\bar{d}$ is taken to be $2.5h$, with h as the nodal spacing.

Example 6.1. First, we consider an exterior Neumann problem whose exact solution is known as [24]

$$u = \frac{1}{r^2}\cos 2\theta = \frac{x_1^2 - x_2^2}{(x_1^2 + x_2^2)^2}, \qquad \text{in } \Omega' = \left\{(x_1, x_2) \in \mathbb{R}^2 : r = \sqrt{x_1^2 + x_2^2} \ge 1\right\}.$$

The boundary condition is

$$\left.\frac{\partial u}{\partial \mathbf{n}}\right|_{\Gamma} = -2\cos 2\theta = 2x_2^2 - 2x_1^2.$$

Table 6.1: Approximations and convergence rates of the solutions for Example 6.1.

x_1, x_2		Numerical solutions				Exact solutions	Rates
		$N = 8$	$N = 16$	$N = 32$	$N = 64$		
1.75, 0.0	u	0.296318	0.318733	0.324541	0.326031	0.326531	1.97
	$\partial u/\partial x_1$	-0.336516	-0.364252	-0.370904	-0.372607	-0.373178	2.00
3.0, 0.0	u	0.101128	0.108458	0.110434	0.110941	0.111111	1.96
	$\partial u/\partial x_1 * 10^1$	-0.673635	-0.723056	-0.736228	-0.739607	-0.740741	1.96
5.0, 0.0	$u * 10^1$	0.364191	0.390450	0.397563	0.399388	0.400000	1.96
	$\partial u/\partial x_1 * 10^1$	-0.145661	-0.156180	-0.159025	-0.159755	-0.160000	1.96
10.0, 0.0	$u * 10^2$	0.910522	0.976125	0.993908	0.998469	1.000000	1.96
	$\partial u/\partial x_1 * 10^2$	-0.182103	-0.195225	-0.198782	-0.199694	-0.200000	1.96

Table 6.2: Approximations and convergence rates of the solutions for Example 6.2.

x_1, x_2		Numerical solutions				Exact solutions	Rates
		$N = 8$	$N = 16$	$N = 32$	$N = 64$		
1.75, 0.0	u	0.336859	0.325887	0.326738	0.326565	0.326531	2.63
	$\partial u/\partial x_1$	-0.352098	-0.372420	-0.373382	-0.373220	-0.373178	2.87
3.0, 0.0	u	0.119442	0.110831	0.111188	0.111123	0.111111	3.03
	$\partial u/\partial x_1 * 10^1$	-0.786835	-0.739109	-0.741238	-0.740818	-0.740741	2.94
5.0, 0.0	$u * 10^1$	0.432246	0.398934	0.400283	0.400042	0.400000	3.07
	$\partial u/\partial x_1 * 10^1$	-0.172626	-0.159581	-0.160112	-0.160017	-0.160000	3.06
10.0, 0.0	$u * 10^2$	1.081415	0.997314	1.000708	1.000105	1.000000	3.07
	$\partial u/\partial x_1 * 10^2$	-0.216262	-0.199463	-0.200142	-0.200021	-0.200000	3.07

Example 6.2. An exterior Neumann problem with exact solution

$$u = \frac{x_1^2 - x_2^2}{\left(x_1^2 + x_2^2\right)^2}, \qquad \text{in } \Omega' = \mathbb{R}^2 \big/ \big([-1,1] \times [-1,1]\big).$$

The two examples have the same exact solutions, but the boundary of Example 6.2 is a polygonal curve that can be approximated exactly.

The comparison of the exact solutions and the numerical solutions with 32 regularly distributed boundary nodes are plotted in Fig. 6.1. It can be clearly seen that the numerical solutions are in excellent agreement with the exact solutions.

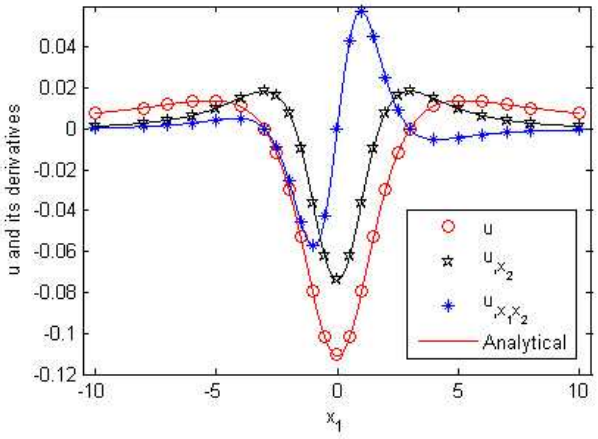

Fig. 6.1. Results of u and its derivatives for Example 6.1 along the line $x_2 = -3$.

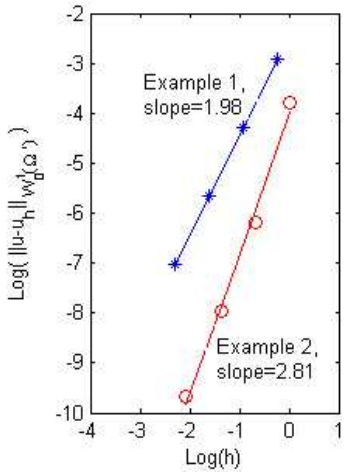

Fig. 6.2. Convergence for Examples 6.1 and 6.2.

To show the convergence of the presented method, regularly distributed 8, 16, 32 and 64 nodes are used. The results of convergence are shown in Fig. 6.2. Besides, the values of the

numerical solutions of the potential u and its derivatives at some inner points are given in Tables 6.1 and 6.2.

As we expected, the results from the proposed meshless method gradually converge to the exact values along with the increase of the boundary nodes. Comparing the numerical results, we can see that the precision and convergence rates of Example 6.2 are higher than those of Example 6.1. The reason for this phenomenon is that the approximation of the boundary of Example 6.1 by cells yields some numerical errors. These observations are in consistency with the error analysis we obtain.

7. Conclusions

In this study, the GBNM has been developed to solve 2-D exterior Neumann problems. In this meshless Galerkin method, the MLS approximations, based on nodes just on the boundary, are implemented to represent the unknown functions; and cells on the boundary are used for numerical integration. Unlike other meshless Galerkin method, the GBNM can reduce the dimensionality of the original problem by one, thus it is especially suitable for the exterior problems. The differences between the GBNM and the Galerkin BEM are as follows. In the GBNM, the boundary nodes are independent of the integration cell structure, but in the Galerkin BEM, the boundary nodes are tightly coupled to the surface element. In the GBNM, the boundary discretization is achieved by the MLS approximation of the nodal data, which does not require an element structure and therefore simplifies mesh generation and problems which require modification of the mesh, such as adaptive refinement. But in the Galerkin BEM, the elements provide a means of subdividing the boundary of a problem; in each element, approximating polynomials are used for the test and trial functions.

The optimal asymptotic error estimates for this method have been derived in Sobolev spaces, which show that the error bound of the numerical solution is directly related to the nodal spacing. The error study shows that the error results mainly from the approximation of the boundary function by the MLS approximations and the approximation of the boundary by the cell structure. Besides, the primary field variables and their successive derivatives hold the same convergence rate. Some numerical experiments have been given to confirm the theoretical results and to show the accuracy of the method.

Since the proposed meshless GBNM does not explicitly involve meshes in modeling of the boundary of domain, this method provides a convenient implementation of adaptive process by simply adding or deleting boundary nodes, which is a future research topic.

Acknowledgments. This work was supported by the Educational Commission Foundation of Chongqing, China (KJ100607 and KJ100621).

References

[1] T. Belytschko, Y. Krongauz, D. Organ, M. Fleming and P. Krysl, Meshless methods: an overview and recent developments, *Comput. Method. Appl. M.*, **139** (1996), 3-47.

[2] S. Li and W.K. Liu, Meshfree Particle Methods, Springer, Berlin, 2004.

[3] P. Krysl and T. Belytschko, Element-free Galerkin method: convergence of the continuous and discontinuous shape functions, *Comput. Method. Appl. M.*, **148** (1997), 257-277.

[4] T. Strouboulis, K. Copps and I. Babuska, The generalized finite element method, *Comput. Method. Appl. M.*, **190** (2001), 4081-4196.

[5] Y.Q. Huang, W. Li and F. Su, Optimal error estimates of the partition of unity method with local polynomial approximation spaces, *J. Comput. Math.*, **24** (2006), 365-372.
[6] C.A. Duarte and J.T. Oden, H-p clouds—an *h-p* meshless method, *Numer. Meth. Part. D. E.*, **12** (1996), 673-705.
[7] R. Cheng and Y. Cheng, Error estimates for the finite point method, *Appl. Numer. Math.*, **58** (2008), 884-898.
[8] Y.X. Mukherjee and S. Mukherjee, The boundary node method for potential problems, *Int. J. Numer. Meth. Eng.*, **40** (1997), 797-815.
[9] G. Li and N.R. Aluru, Boundary cloud method: a combined scattered point/boundary integral approach for boundary-only analysis, *Comput. Method. Appl. M.*, **191** (2002), 2337-2370.
[10] J. Zhang, Z. Yao and H. Li, A hybrid boundary node method, *Int. J. Numer. Meth. Eng.*, **53** (2002), 751-763.
[11] G.R. Liu and Y.T. Gu, Boundary meshfree methods based on the boundary point interpolation methods, *Eng. Anal. Bound. Elem.*, **28** (2004), 475-487.
[12] K.M. Liew, Y. Cheng and S. Kitipornchai, Boundary element-free method (BEFM) and its application to two-dimensional elasticity problems, *Int. J. Numer. Meth. Eng.*, **65** (2006), 1310-1332.
[13] X. Li and J. Zhu, A Galerkin boundary node method and its convergence analysis, *J. Comput. Appl. Math.*, **230** (2009), 314-328.
[14] Lancaster P and Salkauskas K. Surface generated by moving least squares methods, *Math. Comput.*, 1**37** (1981), 141-158.
[15] X. Li and J. Zhu, A Galerkin boundary node method for biharmonic problems, *Eng. Anal. Bound. Elem.*, **33** (2009), 858-865.
[16] X. Li and J. Zhu, A meshless Galerkin method for Stokes problems using boundary integral equations, *Comput. Method. Appl. M.*, **198** (2009), 2874-2885.
[17] G.R. Liu and Z.H. Tu, An adaptive procedure based on background cells for meshless methods, *Comput. Method. Appl. M.*, **191** (2002) 1923-1943.
[18] C.A. Duarte and J.T. Oden, An hp adaptive method using clouds, *Comput. Method. Appl. M.*, **139** (1996) 237-262.
[19] J.L. Lious and E. Magenes, Non-Homogeneous Boundary Value Problems and Applications, Springer, Berlin, 1972.
[20] J. Giroire and J.C. Nedelec, Numerical solution of an exterior Neumann problem using a double layer potential, *Math. Comput.*, **32** (1978), 973-990.
[21] J. Zhu and Z. Yuan, Boundary Element Analysis, Science Press, Beijing, 2009.
[22] R. Dautray and J.L. Lious, Mathematical Analysis and Numerical Methods for Science and Technology, Integral Equations and Numerical Methods, vol. 4, Springer, Berlin, 2000.
[23] M.N. Le Roux, Methode d'éléments finis pour la résolution numérique de problèmes extérieurs en dimension 2, *RAIRO Anal. Numer.*, **11** (1977), 27-60.
[24] D. Yu, Mathematical Theory of Natural Boundary Element Method, Science Press, Beijing, 1993.
[25] J. Zhu and S. Zhang, Galerkin boundary element method for solving the boundary integral equation with hypersingularity, *J. Univ. Sci. Technol. China*, **37** (2007), 1357-1362.
[26] J.C. Nedelec, Finite element for the exterior problems using integral equations, *Int. J. Numer. Meth. Fl.*, **7** (1987), 1229-1234.